



Removal of methylene blue from aqueous solution by coconut coir dust as a low-cost adsorbent

Abdullah Al Ashik¹ · Md. Ataur Rahman¹ · Debadas Halder² · Md. Mufazzal Hossain¹

Received: 8 July 2020 / Accepted: 6 February 2023 / Published online: 24 February 2023
© The Author(s) 2023

Abstract

Adsorption of methylene blue (MB) from its aqueous solution onto coconut coir dust was studied in batch method. Coconut coir dust was characterized before and after adsorption by FT-IR spectroscopy and scanning electron microscopy (SEM). Surface charge, pH_{zpc} of the adsorbent was measured by the method suggested by Huang and Ostovic and was found to be 7.65 (± 0.05). Batch kinetic experiments were performed and effects of several operational parameters i.e., contact time, initial concentration, pH of the solution and temperature on adsorption process were investigated. The effect of pH on adsorption was examined using a MB solution of 31.98 mg L⁻¹ at 30 °C on coconut coir dust varying the pH range from 3.02 to 11.04. At basic condition, the uptake increased significantly and reached the maximum at pH 9.0. The batch adsorption model, based on the assumptions of the Lagergren's pseudo-first order and the Ho's pseudo-second order model were applied to investigate the kinetics of this adsorption process. The results showed that the kinetic data fit very well to the pseudo-second order kinetic model. The adsorption isotherms were determined at four different particle sizes which ranges from < 106 to 300 μm . Among them < 106 μm particle size was chosen for whole process because of comparatively good adsorption capacity. The adsorption isotherms at different temperatures maintaining pH at 7.68 were studied and results show that the amount adsorbed increases with the increase in the temperature under all conditions. The linear correlation coefficients indicate that the Langmuir isotherm best fitted with the experimental data. Thermodynamic parameters such as Gibbs free energy change (ΔG), enthalpy change (ΔH) and entropy change (ΔS) were calculated. The values of ΔH and ΔS were found to be +30.16 kJ mol⁻¹ and +0.128 kJ mol⁻¹ K⁻¹, respectively. At pH 7.68, the present system was spontaneous and endothermic in nature. It was found that when the temperature was increased from 303 to 333 K, the ΔG value decreased.

Keywords Adsorption · Bioadsorbent · Coconut coir dust · Adsorption kinetics

Introduction

The expansion of industrialization is changing the lifestyle of human beings and greatly impacting the surroundings of the habitants. Today, the health of mammals and aquatic lives are becoming the prime concern. Industrial effluents containing toxic chemicals mainly dyes and pigments are greatly accumulating in the environment and causing serious harm (Noroozi et al. 2008; Sturm et al. 1975). In most cases, these toxic chemicals make their ways into the river.

These dyes are highly soluble in water and reduce the oxygen level in water. This feature greatly hampers the aquatic lives, consequently affect the biodiversity. Dyes in wastewater cause aesthetic problems also they absorb and scatter sunlight, thus harm the aquatic ecosystem (Ghaedi et al. 2013). Most of the industrial effluents are capable of preventing photosynthesis process of aquatic plants by blocking the penetration of sunlight into water. Some azo dyes can produce potentially carcinogenic aromatic amines by metabolic cleavage of the azo linkage. In addition, most dyes and pigments have detrimental effects toward microorganism and directly inhibit or destroy their catalytic efficiency (Ghaedi et al. 2013). Such as, prokaryotes and diazotrophs play a role in nitrogen fixation hence nitrogen cycle (Santos et al. 2012), are very sensitive toward toxic chemicals and lose their nitrogen fixation capacity. Recent investigation reveals that some of these dyes are carcinogenic and have adverse

✉ Md. Ataur Rahman
ataur@du.ac.bd

¹ Department of Chemistry, University of Dhaka, Dhaka 1000, Bangladesh

² Institute of Education and Research, University of Dhaka, Dhaka 1000, Bangladesh

effect on neurological system and respiratory system (Yahagi et al. 1975; Barbosa and Peters 1971; Reyes et al. 1996). Therefore, it is very necessary to remove dyes and pigments for aqueous industrial effluents prior to exposal. A number of techniques have been adopted for the treatment of industrial effluents, such as chemical precipitation, ion exchange, electrochemical treatment, flocculation, reverse osmosis, ozonation, photodegradation, coagulation and adsorption (Guo et al. 2013; Schoonenberg Kegel et al. 2010; Qi et al. 2015; Asfaram et al. 2016). Most of the methods are efficient but expensive. Adsorption is considered as cost effective, efficient and promising technique for its ease of operation and wide range of application (Li et al. 2015). Recently, bio-adsorbents, adsorbents based on biological materials such as agricultural waste, byproducts and plant stems have been extensively studied to remove dye molecules from water. Sunflower seed hull (Hameed 2008), sugarcane bagasse (Zhang et al. 2011), *Luffa cylindrica* fibers (Kesraoui et al. 2016), pineapple leaf (Rahmat et al. 2016) are used as bio-adsorbent to remove different types of dyes from its aqueous solution. Researchers reported that these bioadsorbents are very efficient with high porosity and large surface area, cost effective and available to remove organic pollutants from water (Bhatnagar et al. 2010). In present investigation, coconut coir dust (CCD) is used as bioadsorbent to remove a model dye, methylene blue (MB) from its aqueous solution. Lim et al. (Lim et al. 2017) and Brito et al. (BrITO and Andrade 2010) investigated the adsorption of MB on breadnut peel and Brazil nutshell, respectively. These bio-adsorbents are not much available in Bangladesh but CCD is very available as domestic waste. It is a natural polysaccharide which contains lignin, cellulose, hemicelluloses and other extractives. The objective of the present investigation is to prepare an efficient, cost effective bioadsorbent for the adsorption study that comprises the effect of different operational parameters on the adsorption process. Mechanism and kinetics of adsorption will also be investigated. Along with these, applicability of adsorption isotherm for this process and information of thermodynamic parameters for its thermodynamic feasibility will give extensive illustration about this adsorption process. All these are in agreement with the application of this material as an efficient bioadsorbent for the treatment of industrial hazardous effluents.

Materials and methods

The analytical grade chemicals are used for the study and the chemicals were obtained from Fluka, Germany. All the solutions were prepared and their further dilutions were carried out by using deionized water. MB, chemical formula $C_{16}H_{18}ClN_3S$ was used as a model adsorbate. pH of the solution was adjusted using 0.01 M HCl and 0.01 M NaOH

solution, and was measured using pH meter (JENWAY 3510 pH meter). Thermostated waterbath shaker (OLS200, Grant) was used for batch adsorption process. The supernatant solution was centrifuged by a centrifuge machine (Centurion scientific).

Preparation of adsorbent

Two medium sized coconuts collected from local market of Dhaka, Bangladesh. CCD was extracted from these coconuts and dipped into deionized water for 3 days to soak. After that, it was washed several times with water until all the colored extract was removed. It was oven dried at 60 °C for 24 h. Then the dried coconut coir was blended. The blended coconut coir was sieved using 106 µm, 150 µm, 212 µm, and 300 µm sieve to obtain particles in these ranges. Each sized of this particle was stored in a different reagent bottle prior to use for adsorption studies. CCD was not treated physically or chemically prior to adsorption experiments.

Adsorption studies

The adsorption study of MB on CCD was carried out by the batch equilibrium method. A fixed amount of CCD was suspended in 100 mL of various initial concentrations of the MB solution in a stoppered 100 mL reagent bottle and maintained under isothermal conditions at 150 rpm. The equilibrium time for this adsorption process was experimentally determined and found to be 60 min. Previous study reports that the adsorption of MB on breadnut peel also reaches equilibrium within 60 min (Lim et al. 2017). After adsorption, the resultant supernatant solution was centrifuged at 4000 rpm for 10 min. The concentration of MB in the centrifugate after adsorption was determined spectrophotometrically at 664 nm.

The percentage of MB dyes adsorbed was calculated using the following equation

$$\text{Adsorption (\%)} = 100 \times (C_o - C_e) / C_o,$$

C_o and C_e are the initial and equilibrium concentrations of MB.

Equilibrium amount adsorbed (mg g^{-1}) was calculated using the following equation

$$q_e = (C_o - C_e) V / W,$$

V is the volume of solution and W is the amount of CCD in g.

Kinetics of adsorption was also investigated. For this study, a fixed amount of CCD was suspended in 100 mL of various initial concentrations of MB solution in a stoppered 100 mL reagent bottle and maintained under isothermal conditions at 150 rpm. Then, after certain time intervals about

2 mL of supernatant solution was taken in a semi-micro test tube and analyzed as the above process.

Determination of zero point charge (pH_{zpc}) of adsorbent

The zero point charge (pH_{zpc}) of solid CCD surface was determined by the method suggested by Huang and Ostovic (Huang and Ostovic 1978; Bowers and Huang 1980). 40 mL 0.01 M NaCl solution of pH 7 was taken in each of four different reagent bottles. Then, 0.1 g of the adsorbent was added to each bottle and mixed. The mixtures were agitated in thermo-mechanical shaker for about 24 h. Two bottles of suspension were titrated directly with 0.05 M HCl and 0.05 M NaOH solution separately using micro burette (± 0.01 mL). During the titration, the pH reading was recorded cautiously. The supernatants of other two bottles after filtration were titrated with HCl and NaOH solutions as described above. This procedure was also carried out using 0.001 M NaCl solution.

Characterization of the adsorbent

Coconut coir dust after and before adsorption was characterized by FTIR spectrophotometer (FTIR 8400S, Shimadzu) and scanning electron microscope (JSM6490LA). A very tiny amount of prepared CCD before and after adsorption was mixed separately with KBr in ratio of 0.1:100 and grinded in an agate mortar. A pellet of the grinding mixture was prepared by pressing with hydraulic pressure. Then a FTIR spectrum was taken of the prepared pellets. The FTIR spectrum of MB was also recorded in the same way. For SEM analysis, a small amount of CCD surface was put on the conducting tape which makes conduction between the sample and the stub. Then SEM image of solid surface of CCD was taken before and after adsorption.

Results and discussion

Determination of pH_{zpc} of adsorbent

The pH at which surface charge of CCD is zero has been determined. Results are presented in Fig. 1a and b. The pH_{zpc} value of CCD has been found to be 7.55 and 7.75 in 0.01 M and 0.001 M NaCl solution, respectively. The average value of pH_{zpc} is $7.65 (\pm 0.05)$. So, the surface of CCD is positively charged below pH_{zpc} . Acidic water donates H^+ to the surface hence the surface becomes protonated and positively charged. The positively charged surface attracts anions. On the other hand, the surface is negatively charged above pH_{zpc} as the surface becomes deprotonated and hence the surface attracts cations (Anirudhan et al. 2009).

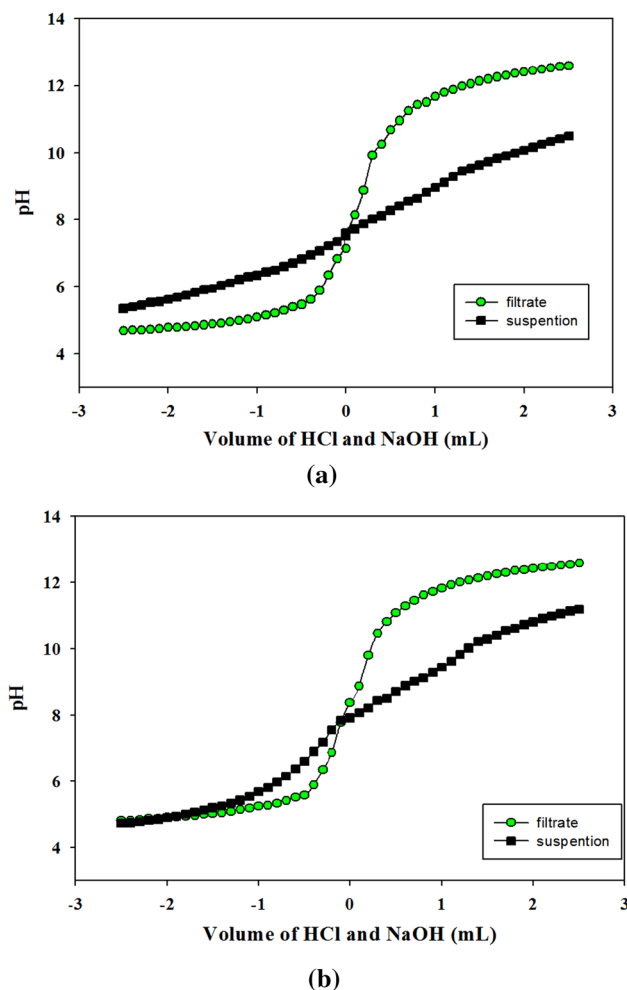


Fig. 1 **a** A pH metric titration curve of coconut coir dust in 0.01 M NaCl solution. **b** A pH metric titration curve of coconut coir dust in 0.001 M NaCl solution

Optimization of pH

Adsorption capacity of CCD varies with the pH of the suspension. Figure 2 shows the effect of suspension pH on the adsorption efficiency of CCD. The adsorption of MB increases from 51.3% at pH 3.02 to 85.8% at pH 9.0. Lower percentage of adsorption of MB at highly acidic pH may be due to the presence of excess H^+ (proton) ions in the medium. These highly mobile protons compete with MB cations and functional groups such as the amine (NH_2^+) group in CCD for the available adsorption sites (Senthil Kumar et al. 2010). As the suspension pH increase, the number of negatively charged adsorption sites on the CCD increase, which may result in the increase in adsorption of cationic MB molecules. These increase in adsorption is due to the electrostatic force of attraction between negatively charged adsorption sites and cationic MB molecules (Qin et al. 2009). Adsorption of MB on breadnut peel and Brazil

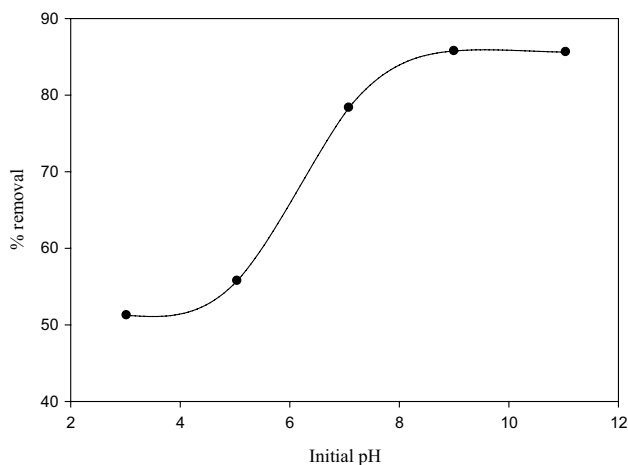


Fig. 2 Plot of percentage removal against initial pH for adsorption of aqueous methylene blue solution on coconut coir dust at 30 °C

nutshell also show the same results (Lim et al. 2017; Brito and Andrade 2010). Adsorption decreases with decreasing pH and increases with increasing pH. Both breadnut peel

and Brazil nutshell show substantial amount of adsorption at on and above neutral pH like CCD.

Study of adsorption kinetics

Lagergren’s pseudofirst order equation and Ho’s pseudo-second order equation were employed to investigate the adsorption kinetics onto CCD shown in Fig. 3a and b, respectively. The values of rate constants, regression coefficients and percentage deviation of q_e comparing the experimental values and the values calculated from pseudofirst order and pseudosecond order plots are given in Tables 1 and 2. However, it was observed that the experimentally obtained q_e values significantly deviate from the values determined from the Lagergren plot of pseudofirst order kinetic model. Therefore, the pseudofirst order kinetic model inefficient to describe the adsorption phenomenon of MB on CCD.

On the other hand, experimentally determined q_e values match with that obtained from the pseudosecond order kinetic model with small deviation as well as their regression factor (R^2) values are very close to unity. Therefore, it is evident that pseudosecond order kinetic model provide good

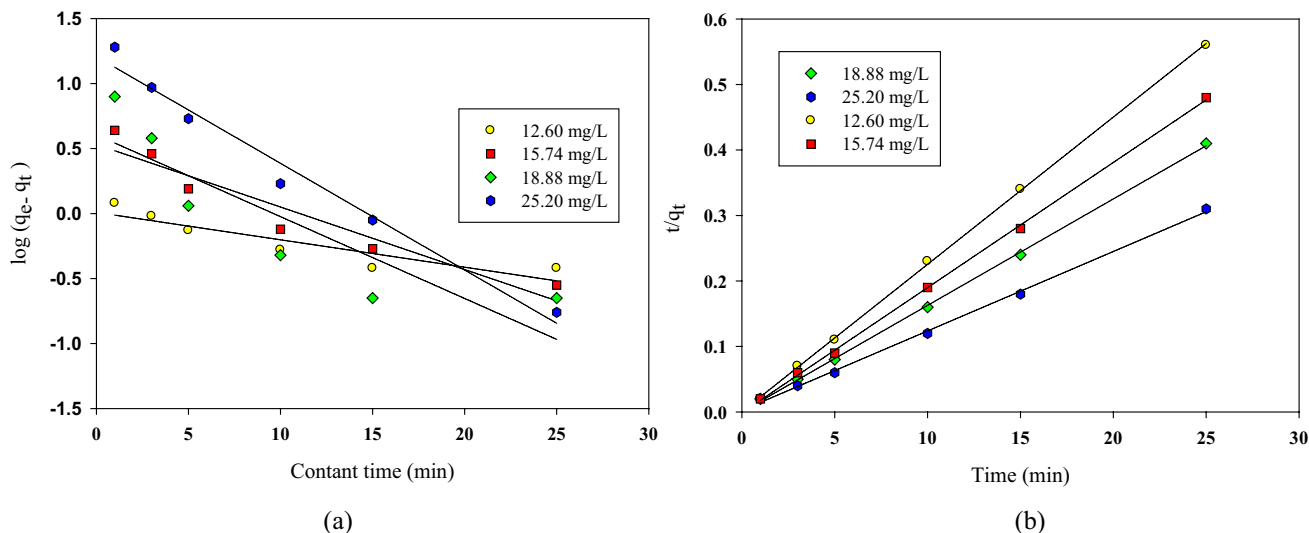


Fig. 3 a Plot of $\log (q_e - q_t)$ versus contact time to investigate the pseudo-first order kinetics for adsorption of methylene blue solutions on coconut coir dust. **b** Plot of t/q_t versus time to investigate the

pseudo-second order kinetics for adsorption of methylene blue solutions on coconut coir dust

Table 1 Computed data from Fig. 3a for q_e and k_1 of pseudo-first order kinetics for adsorption of methylene blue on coconut coir dust at 30 °C

Initial conc. (mgL ⁻¹)	R_2	Pseudo-first order constant, k_1 (min ⁻¹)	q_e (computed) mg g ⁻¹	q_e (experimental) mg g ⁻¹	Percentage deviation of q_e
12.60	0.8208	4.86×10^{-2}	1.02	44.94	97.73
15.74	0.9122	11.07×10^{-2}	3.40	52.37	93.50
18.88	0.7646	14.48×10^{-2}	4.03	60.95	93.38
25.20	0.9781	18.88×10^{-2}	16.09	79.98	79.98

Table 2 Compute data from Fig. 3b for q_e and k_2 of pseudo second-order kinetics for adsorption of methylene blue on coconut coir dust at 30 °C

Initial conc. (mgL ⁻¹)	R_2	Pseudo-second order rate constant, k_2 (gmg ⁻¹ min ⁻¹)	q_e (computed) mg g ⁻¹	q_e (experimental) mg g ⁻¹	Percentage deviation of q_e
12.60	0.9997	42.19×10^{-2}	44.44	44.94	1.11
15.74	0.9995	14.03×10^{-2}	52.35	52.37	0.03
18.88	0.9995	66.42×10^{-2}	61.34	60.95	-0.64
25.20	0.9985	3.05×10^{-2}	82.64	79.98	-3.32

correlation for this adsorption process in contrast to pseudo-first order kinetic model. The previous studies (Lim et al. 2017; Brito and Andrade 2010) also report that adsorption of MB on bioadsorbents like, breadnut peel and Brazil nutshell follow pseudo-second order kinetics. The values of pseudo-second order rate constants for different initial concentration of 12.60, 15.74, 18.88 and 25.20 mg L⁻¹ are 42.19×10^{-2} , 14.03×10^{-2} , 66.42×10^{-2} , 3.05×10^{-2} gm g⁻¹ min⁻¹, respectively.

Study of intraparticle diffusion model

The adsorbed molecules can diffuse from one adsorption site another adsorption site on the adsorbent. This diffusion in the adsorption process is checked by fitting the experimental data in intraparticle diffusion model (Wu et al. 2009) proposed by Weber. The plot q_t versus $t^{1/2}$ shows different features with the presence of various diffusions of adsorbate. The model explains that the initial linear region in the plot can be attributed to film diffusion process, governed by boundary layer effect. The second parallel line refers to the intraparticle diffusion stage. The final gradual increase and stable line bear the evidence of pore diffusion mechanism. From Fig. 4, it can be said that the adsorption of low concentration such as 12.60, 15.74, 18.88 mg L⁻¹ MB by CCD cannot properly be described by using intraparticle diffusion model. Hence, adsorption processes at low concentrations usually do not involve the diffusion of adsorbed molecules on the surface of the adsorbent. But comparatively higher concentration like 25.20 mg L⁻¹ is well-fitted for intraparticle diffusion model and the graph clearly shows three stages of diffusion. These features of graph indicate that at high concentration adsorption process undergoes film diffusion, intraparticle diffusion and pore diffusion of adsorbed molecules on the adsorbent surface. The correlation coefficient (R^2) values and obtained values of K_{id} also bear the evidence in support of these results.

Effect of particle size on adsorption isotherm

Adsorption isotherm of MB on CCD of different average particle size < 106, 106–150, 151–212, 213–300 μm was studied at 30 °C and pH 7.68 with different initial MB

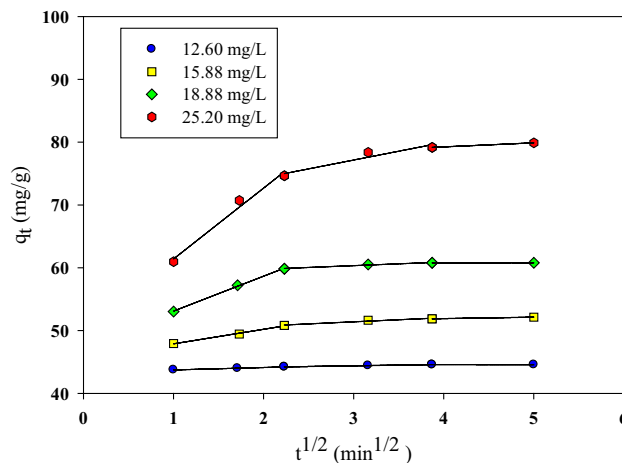


Fig. 4 Plot of q_t versus $t^{1/2}$ for investigating the intraparticle diffusion mechanism for adsorption of different concentration of methylene blue solutions on coconut coir dust

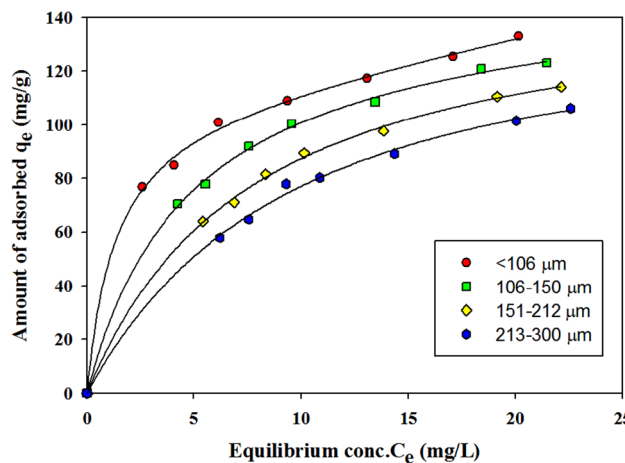


Fig. 5 Comparison of adsorption isotherms of methylene blue on coconut coir dust with different particle sizes

concentrations and the results are shown in Fig. 5. It is observed that the amount of adsorbed increase with decreasing average particle size. The similar trend was observed for the variation of particle size in the previous research work (Ahmed and Rahman 2021). This can be ascribed as the active surface area of larger particles is lower than that of

smaller particles. The small sized particles have more internal porous structure than the larger sized particles of CCD. Hence, the adsorption of MB increases for relative small particles of adsorbent. For larger particles, active surface area is small and also diffusion is less compared to small particles. Hence most of the adsorption sites of internal surface of larger particles may remain unoccupied and consequently, the amount of dye adsorbed is small.

Effect of temperature on adsorption isotherm

A plot of amount of adsorbed (q_e) as a function of time at various temperatures is shown in Fig. 6. The figure clearly states that the amount of MB adsorbed on CCD increased with increasing temperature from 303 K (30 °C) to 333 K (60 °C). It is also observed from the figure that the change of amount of adsorbed (q_e) is very slight with varying temperature. In all conditions, adsorption increase with the increase in equilibrium concentration of MB and other bioadsorbents also follow the same trend (Mittal et al. 2013).

Study of adsorption isotherm model

Adsorption isotherms were constructed at four different temperatures using MB solutions of initial pH of 7.68 shown in Fig. 7a–c, and results are presented in Tables 3, 4 and 5. Langmuir, Freundlich, Temkin isotherm models have a good correlation coefficient with the experimental data ($R^2 > 0.90$). However, Langmuir isotherm had the highest correlation coefficient (0.9954–0.9986), thus Langmuir isotherm model can be considered as the best among the models although others models can also be used to account for the adsorption process. Lim et al. also report that adsorption

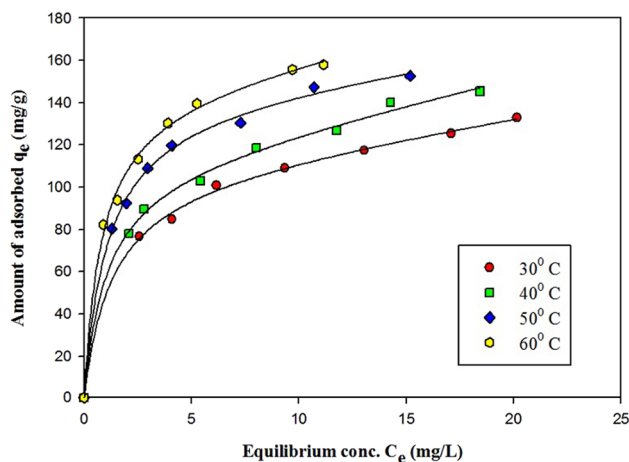


Fig. 6 Plots of adsorption isotherms for adsorption of aqueous methylene blue solution on coconut coir dust at different temperature and pH 7.68

of MB onto breadnut peel best fits in Langmuir isotherm model and support our finds (Lim et al. 2017).

This adsorption system well fitted with Langmuir isotherm model which means monolayer adsorption occurs. So, the adsorbent, CCD has a finite capacity for the MB molecules and beyond this capacity the adsorption process reaches to an equilibrium where no further adsorption seems to occur. The values of Langmuir adsorption constant (K_L) and maximum adsorption capacity (q_m) increase with temperature which indicates an increase in the binding force of the adsorbate molecule onto the adsorbent.

Heat of adsorption and other thermodynamic parameters

Gibbs free energy, enthalpy and entropy change (ΔG , ΔH and ΔS) for the adsorption process were calculated from the experimental observation (Fig. 8) using the equations below and the value presented in Table 6.

$$\ln(q_e/C_e) = \Delta S/R - \Delta H/RT$$

$$\Delta G = \Delta H - T\Delta S$$

where q_e/C_e is known as the adsorption affinity (Du et al. 2007; Sarma et al. 2008). The values of ΔH and ΔS were calculated from the slope and intercept of the linear plot of $\ln(q_e/C_e)$ versus $1/T$ (Fig. 8) and the equation was utilized to obtain ΔG . The value of enthalpy of adsorption (ΔH) was found to be +30.16 kJ mol⁻¹. The positive value of enthalpy of adsorption indicates that the adsorption process was endothermic and hence, increase in temperature favors the interaction between MB molecules and CCD surface. The enthalpy change within the ranges of 10–40 kJ mol⁻¹ and 40–1000 kJ mol⁻¹, indicates physisorption and chemisorption process, respectively (McCash 2001). The ΔH value of this study is within the ranges of the physisorption process. The value of ΔS found to be +0.128 kJ mol⁻¹ K⁻¹. Similarly, the positive value of ΔS suggests the increase in randomness at the solid (CCD)-liquid (MB) interface during the adsorption. The entropy can increase as water molecule could replace the hydrated dye ions from the adsorption sites on adsorbent and also this increase in entropy indicates the possibility of fragmentation of dye molecules after adsorption (Messina and Schulz 2006). The fragmentations may remain in the bulk of the suspension and contribute to increase in entropy. The values of ΔG were calculated from the values of ΔH and ΔS and tabulated in Table 6. The values of Gibbs free energy (ΔG) are negative and decrease with the increase in temperature from -8.62 to -12.46 kJ mol⁻¹ which suggests that the adsorption is spontaneous process and more favorable at high temperature (Lim et al. 2017).

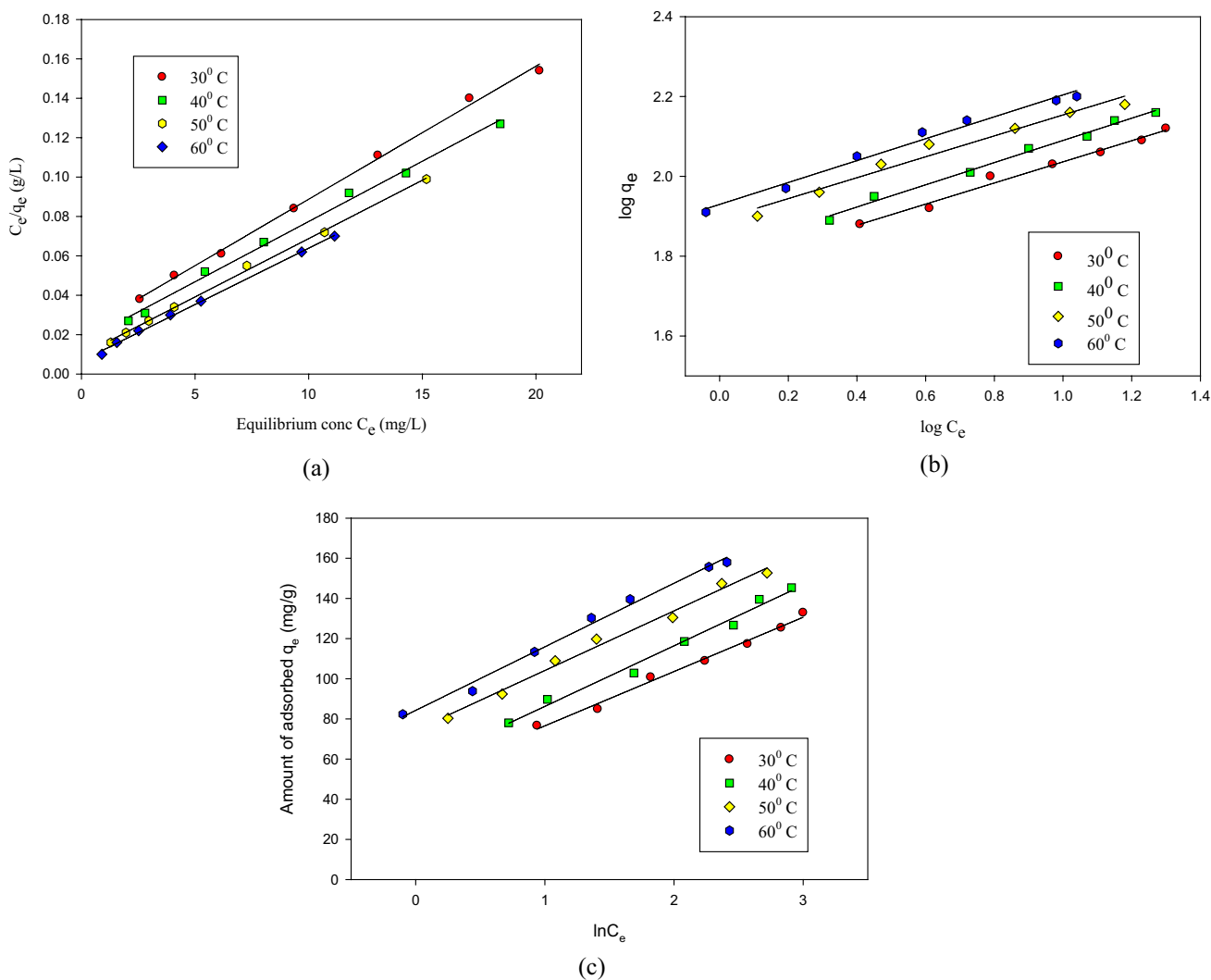


Fig. 7 **a** Plot of C_e/q_e versus C_e to investigate the feasibility of Langmuir isotherm for adsorption of methylene blue on coconut coir dust with varying temperature. **b** Plot of $\ln q_e$ versus $\ln C_e$ to investigate the feasibility of Freundlich isotherm for adsorption of methylene blue on

coconut coir dust with varying temperature. **c** Plot of $\ln q_e$ versus $\ln C_e$ to investigate the feasibility of tempkin isotherm for adsorption of methylene blue on coconut coir dust with varying temperature

Table 3 Langmuir isotherm parameters for adsorption of methylene blue on coconut coir dust with varying temperatures

Temperature (°C)	R^2	Langmuir adsorption constant, K_L (L mg ⁻¹)	Maximum adsorption capacity, q_m (mg g ⁻¹)
30	0.9975	47.17	147.65
40	0.9954	61.72	163.93
50	0.9986	105.26	169.49
60	0.9983	149.25	175.43

Table 4 Freundlich isotherm parameters for adsorption of methylene blue on coconut coir dust with varying temperature

Temperature (°C)	R^2	Freundlich isotherm constant, K_F (dm ³ g ⁻¹)	Intensity of adsorption N
30	0.9857	59.10	0.2646
40	0.9908	64.84	0.2779
50	0.9697	77.89	0.2619
60	0.9842	84.98	0.2743

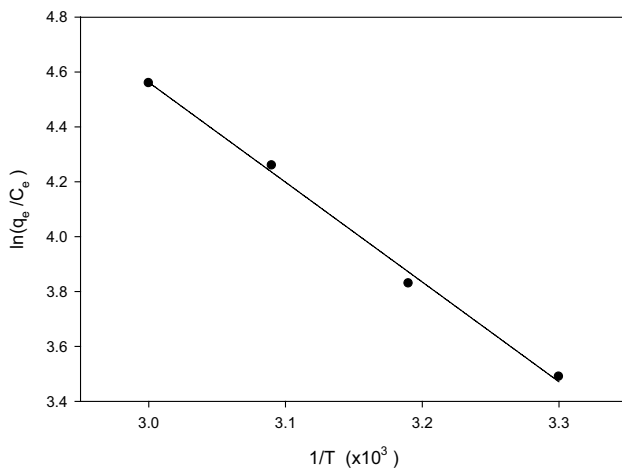
Analysis of FT-IR spectrum

The FT-IR spectrum of MB is shown in Fig. 9a. The broad band between 3600 and 3200 cm⁻¹ is observed in the

spectrum of methylene blue and it is assigned to stretching vibrational of several hydroxyl group of moisture. An intense band observed in the region of 1598.99 cm⁻¹ was due to C=C stretching of aromatic ring of MB. The peak

Table 5 Temkin isotherm parameters for adsorption of methylene blue on coconut coir dust with varying temperature

Temperature (°C)	R^2	Tempkin isotherm constant, B ($\text{dm}^3 \text{g}^{-1}$)	Intensity of adsorption A
30	0.9905	27.0388	6.2374
40	0.9865	30.1593	6.4149
50	0.9890	29.6821	12.2521
60	0.9916	31.6596	14.2736

**Fig. 8** Plot of $\ln(q_e/C_e)$ versus $1/T$ ($\times 10^3$) for adsorption of aqueous methylene blue on coconut coir dust with varying temperature**Table 6** Data for estimating the thermodynamic parameters for adsorption of methylene blue on coconut coir dust

Temperatures (K)	ΔH (kJ mol^{-1})	ΔS ($\text{kJ mol}^{-1} \text{K}^{-1}$)	ΔG (kJ mol^{-1})
303	+30.16	+0.128	-8.62
313			-9.90
323			-11.18
333			-12.46

appeared at approximately 1350 cm^{-1} due to C–H bending vibration of methyl group. A signal at 1145.72 cm^{-1} indicates the presence of C–N stretching.

Figure 9b shows the FT-IR spectrum of CCD before adsorption. A broad peak around $3600\text{--}3200 \text{ cm}^{-1}$ is observed in the spectrum and it is assigned to stretching vibration of several hydroxyl groups either from cellulose, hemicelluloses or lignin. The band around $2920\text{--}2923 \text{ cm}^{-1}$ represents the sp^3 C–H stretching of the polymer. A band at 1750 cm^{-1} denotes the C=O stretching of ester or carboxylic groups in carbohydrates. A band appeared at approximately $1425\text{--}1250 \text{ cm}^{-1}$ is due to bending vibration of C–H of

methyl group. The peak around $1165\text{--}1034 \text{ cm}^{-1}$ indicates the presence of C–O–C bonding in the molecule.

The FT-IR spectrum of CCD after adsorption is shown in Fig. 9c and comparison among these three individual spectra is represented in Fig. 9d. The spectra have a number of peaks, indicating the presence of lots of functional groups and molecules in CCD. The strong peak at 1619.3 cm^{-1} can be attributed to the presence of conjugate C–C bond. The strong absorption at 1377.2 cm^{-1} is evident of weak asymmetric vibration of the aliphatic N–O group. The presence of C–O bond of carboxylic acid group shows a peak at 1258.6 cm^{-1} . The peaks at $1060\text{--}1110 \text{ cm}^{-1}$ appear for the presence of C–O bond of alcohol and C–N bond of primary amine ($-\text{NH}_2$) in the structure. The adsorption capacity of adsorbents depends upon available adsorption sites, porosity and interactions of functional groups at the surface. These interactions create an imbalance between forces at the surface and leads to adsorption of molecules at the surface by the van der Waals force. Due to these interactions, the functional groups at the surface are modified to some extent. The peak of CCD at 1714.72 cm^{-1} and 1537.27 cm^{-1} disappear completely after adsorption. However, most of the peaks show a shift in wavenumber which indicate the involvement of the functional groups of CCD in the adsorption process.

Characterization of CCD by SEM

Figure 10 represents the scanning electron microscopy (SEM) photographs of the prepared CCD before and after adsorption. SEM photographs with different magnifications shows the fibrous structure of CCD surface. The walls of the fibers are fractured and there are enormous cavities and pores in the walls which are the factors behind high adsorption capacity. From those figures we can also compare the CCD surface before and after adsorption. The dye molecules should predominantly be adsorbed onto the cavities and pores on the surface, and the cavities and pores are supposed to be covered. So, the surface heterogeneity might be reduced and the surface become more homogeneous (Arami et al. 2005).

Conclusion

The results of this study show that CCD is an effective low-cost adsorbent for the adsorption of typical model dye, MB from its aqueous solution. The adsorbent, CCD has good adsorption capacity for MB and adsorption increases with the increase in dye concentration. Experimental data show that the adsorption process best fitted with Langmuir adsorption isotherm with high linear correlation coefficient values. The isotherm investigation data shows that the adsorption process well fitted with Langmuir isotherm model. The

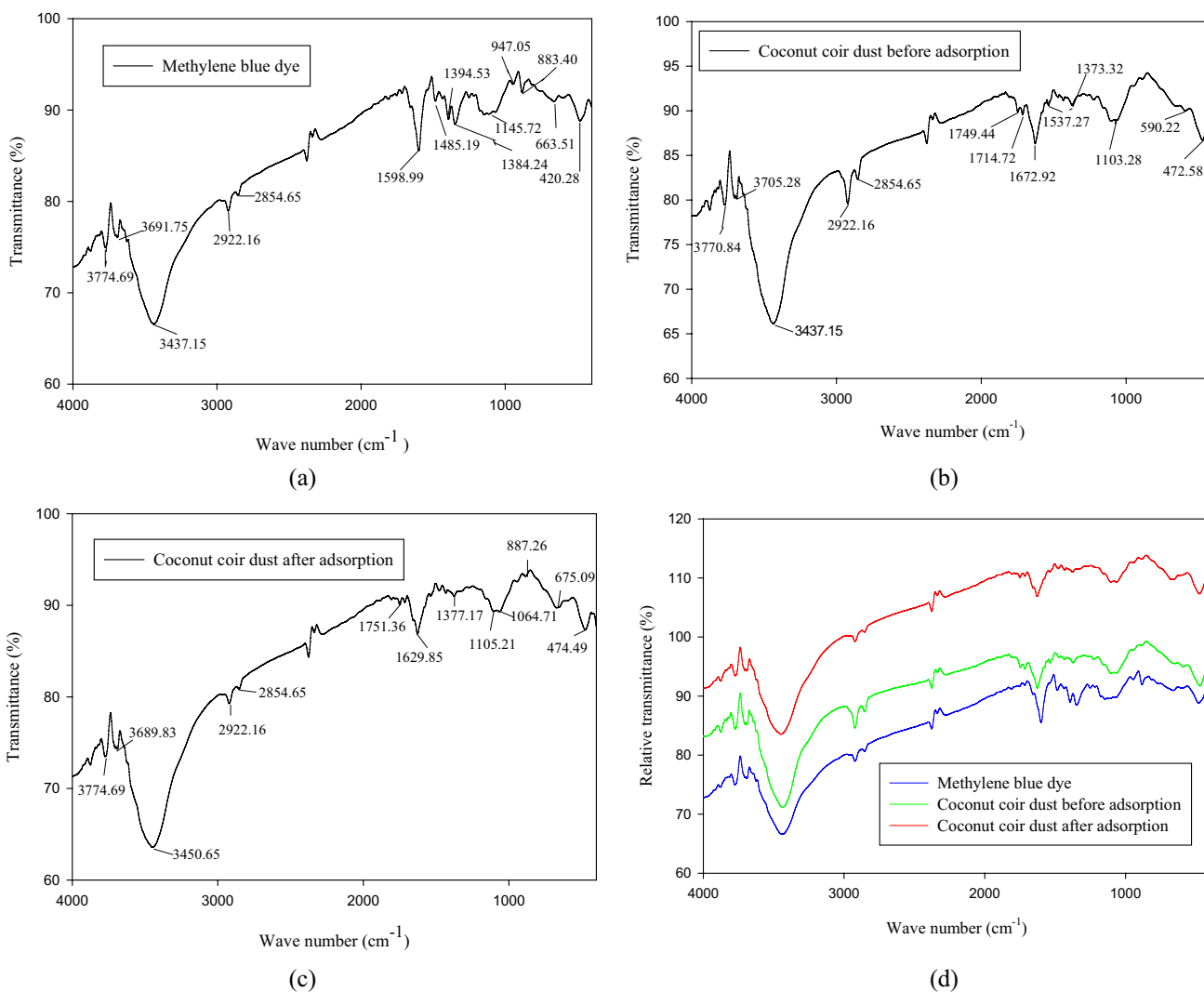
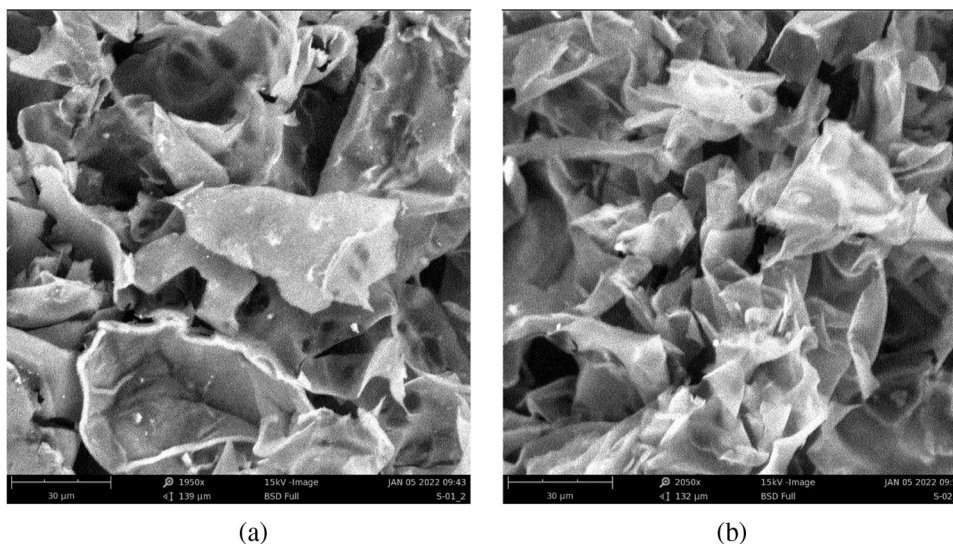


Fig. 9 **a** FT-IR spectrum of methylene blue dye. **b** FT-IR spectrum of coconut coir dust before adsorption. **c** FT-IR spectrum of coconut coir dust after adsorption. **d** Comparison of FT-IR spectrum of meth-

ylene blue dye, coconut coir dust before adsorption and coconut coir dust after adsorption

Fig. 10 SEM micrograph of coconut coir dust before adsorption **(a)** and after adsorption, respectively **(b)**.



adsorption kinetic data indicates that the adsorption process was best described by the pseudo-second order kinetic model. Thermodynamic studies represent the adsorption process as endothermic and spontaneous, and favored at high temperature. Hence, CCD could find its way to industrial application for the treatment of industrial effluents containing dyes.

Funding The research work was not funded by anyone.

Declarations

Conflict of interest On behalf of all authors, the corresponding author states that there is no conflict of interest.

Open Access This article is licensed under a Creative Commons Attribution 4.0 International License, which permits use, sharing, adaptation, distribution and reproduction in any medium or format, as long as you give appropriate credit to the original author(s) and the source, provide a link to the Creative Commons licence, and indicate if changes were made. The images or other third party material in this article are included in the article's Creative Commons licence, unless indicated otherwise in a credit line to the material. If material is not included in the article's Creative Commons licence and your intended use is not permitted by statutory regulation or exceeds the permitted use, you will need to obtain permission directly from the copyright holder. To view a copy of this licence, visit <http://creativecommons.org/licenses/by/4.0/>.

References

- Ahmed N, Rahman MA (2021) Adsorptive removal of 2, 4-dichlorophenol from aqueous solution by using used black tea leaves. *J Mex Chem Soc* 65(2):225–236
- Anirudhan TS, Sreekumari SS, Bringle CD (2009) Removal of phenols from water and petroleum industry refinery effluents by activated carbon obtained from coconut coir pith. *Adsorption* 15:439–451
- Arami M, Limaee NY, Mahmoodi NM, Tabrizi NS (2005) Removal of dyes from colored textile wastewater by orange peel adsorbent: equilibrium and kinetic studies. *J Colloid Interface Sci* 288(2):371–376
- Asfaram A, Ghaedi M, Ghezalbash GR, Dil EA, Tyagi I, Agarwal S, Gupta VK (2016) Biosorption of malachite green by novel biosorbent *Yarrowia lipolytica isf7*: application of response surface methodology. *J Mol Liq* 214:249–258
- Barbosa P, Peters TM (1971) The effects of vital dyes on living organisms with special reference to methylene blue and neutral red. *Histochem J* 3(1):71–93
- Bhatnagar A, Vilar VJP, Botelho CMS, Boaventura RAR (2010) Coconut-based biosorbents for water treatment—a review of the recent literature. *Adv Colloid Interface Sci* 160(1–2):1–15
- Bowers AR, Huang CP (1980) *Prog Wat Tech* 12:629–650
- Brito SMO, Andrade HMC (2010) Brazil nut shells as a new biosorbent to remove methylene blue and indigo carmine from aqueous solutions. *J Hazard Mater* 174:84–92
- Dos Santos PC, Fang Z, Mason SW, Setubal JC, Dixon R (2012) Distribution of nitrogen fixation and nitrogenase-like sequences amongst microbial genomes. *BMC Genom* 13(1):162
- Du SL, Zhou CS, Yang LQ (2007) Deacidification of adlay seed (*Coix lachryma-jobi* var. *mayuen*) miscella with anion-exchange resin. *J Food Process Eng* 30:729–745
- Ghaedi M, Karimi F, Barazesh B, Sahraei R, Daneshfar A (2013) Removal of reactive orange 12 from aqueous solutions by adsorption on tin sulfide nanoparticle loaded on activated carbon. *J Ind Eng Chem* 19(3):756–763
- Guo X, Cai Y, Wei Z, Hou H, Yang X, Wang Z (2013) Treatment of diazo dye CI reactive black 5 in aqueous solution by combined process of interior microelectrolysis and ozonation. *Water Sci Technol* 67(8):1880–1885
- Hameed BH (2008) Equilibrium and kinetic studies of methyl violet sorption by agricultural waste. *J Hazard Mater* 154(1–3):204–212
- Huang CP, Ostovic FB (1978) Removal of cadmium (II) by activated carbon adsorption. *J Environ Eng Div* 104(5):863–878
- Kesraoui A, Moussa A, Ali GB, Seffen M (2016) Biosorption of alpacide blue from aqueous solution by lignocellulosic biomass: *Luffa cylindrica* fibers. *Environ Sci Pollut Res* 23(16):15832–15840
- Li J, Huang Y, Liu Z, Zhang J, Liu X, Luo H, Ma Y, Xu X, Lu Y, Lin J, Zou J, Tang CJ (2015) Chemical activation of boron nitride fibers for improved cationic dye removal performance. *Mater Chem* 3(15):8185–8193
- Lim LBL, Priyantha N, Tennakoon DTB (2017) Breadnut peel as a highly effective low-cost biosorbent for methylene blue: equilibrium, thermodynamic and kinetic studies. *Arab J Chem* 10:S3216–S3228
- McCash EM (2001) In: *Surface Chemistry*, Oxford University Press, pp 54–56. https://books.google.com/books/about/Surface_Chemistry.html?id=QdJyQgAACAAG
- Messina PV, Schulz PC (2006) Adsorption of reactive dyes on titania–silica mesoporous materials. *J Colloid Interface Sci* 299(1):305–320
- Mittal A, Jhare D, Mittal J (2013) Adsorption of hazardous dye eosin yellow from aqueous solution onto waste material de-oiled soya: isotherm, kinetics and bulk removal. *J Mol Liq* 179:133–140
- Noroozi B, Sorial GA, Bahrami H, Arami M (2008) Adsorption of binary mixtures of cationic dyes. *Dye Pigment* 76(3):784–791
- Qi J, Li X, Zheng H, Li P, Wang H (2015) Simultaneous removal of methylene blue and copper (II) ions by photoelectron catalytic oxidation using stannic oxide modified iron (III) oxide composite electrodes. *J Hazard Mater* 293:105–111
- Qin Q, Ma J, Liu K (2009) Adsorption of anionic dyes on ammonium-functionalized MCM-41. *J Hazard Mater* 162(1):133–139
- Rahmat NA, Ali AA, Salmiati, Hussain N, Muhamad MS, Kristanti RA, Hadibarata T (2016) Removal of Remazol brilliant blue R from aqueous solution by adsorption using pineapple leaf powder and lime peel powder. *Water Air Soil Pollut* 227(4):105
- Reyes FGR, Valim MFCFA, Vercesi AE (1996) Effect of organic synthetic food colours on mitochondrial respiration. *Food Addit Contam* 13(1):5–11
- Sarma J, Sarma A, Bhattacharyya KG (2008) Biosorption of commercial dyes on *Azadirachta indica* leaf powder: a case study with a basic dye rhodamine B. *Ind Eng Chem Res* 47(15):5433–5440
- Schoonenberg Kegel F, Rietman BM, Verliefde ARD (2010) Reverse osmosis followed by activated carbon filtration for efficient removal of organic micropollutants from river bank filtrate. *Water Sci Technol* 61(10):2603–2610
- Senthil Kumar P, Ramalingam S, Senthamarai C, Niranjana M, Vijayalakshmi P, Sivanesan S (2010) Adsorption of dye from aqueous solution by cashew nut shell: studies on equilibrium isotherm, kinetics and thermodynamics of interactions. *Desalination* 261(1–2):52–60
- Sturm RN, Williams KE, Macek KJ (1975) Fluorescent whitening agents: acute fish toxicity and accumulation studies. *Water Res* 9(2):211–219
- Wu FC, Tseng RL, Juang RS (2009) Initial behavior of intraparticle diffusion model used in the description of adsorption kinetics. *Chem Eng J* 153:1–8

- Yahagi T, Degawa M, Seino Y, Matsushima T, Nagao M, Sugimura T, Hashimoto Y (1975) Mutagenicity of carcinogenic azo dyes and their derivatives. *Cancer Lett* 1:91–96
- Zhang Z, Moghaddam L, O'Hara IM, Doherty WOS (2011) Congo red adsorption by ball-milled sugarcane bagasse. *Chem Eng J* 178:122–128

Publisher's Note Springer Nature remains neutral with regard to jurisdictional claims in published maps and institutional affiliations.